

Effects of Corrosion on Ground Support and Corrosion Monitoring Methods

Amy J. Chambers, Metallurgical Engineer M.S.^{1, 2}

Donovan J. Benton, Mining Engineer M.S.¹

Michael A. Stepan, Engineering Technician M.S.¹

Seth A. Finley, Engineering Technician¹

Dominic T. Orr, Mining Engineer B.S., Hecla Mining Co.

¹National Institute for Occupational Safety and Health / Spokane Mining Research Division

²Corresponding author: achambers@cdc.gov; 509-354-8007

Abstract

Corrosion of ground support can lead to falls of ground that pose a significant risk to miner safety. To address this problem, the National Institute for Occupational Safety and Health (NIOSH) is investigating corrosion at the Hecla Mining Company's Greens Creek Mine, located near Juneau, Alaska, USA. Field studies have used photogrammetry surveys to document welded-wire mesh corrosion, and laboratory studies at NIOSH's Spokane Mining Research Division (SMRD) have investigated the effects of corrosion on ground support integrity. Findings show that (1) corrosion monitoring through photogrammetric methods may be effective for qualitative measurements of welded-wire mesh corrosion, and (2) there is a relationship between loss of load-bearing capacity and the diameter loss due to corrosion in welded-wire mesh. Photogrammetry results thus far have measured an apparent bulking of the corroded welded-wire mesh, and preliminary laboratory tests have investigated the relationship between the larger bulked and effective wire diameter. If this relationship is verified, these results may indicate that photogrammetry, when combined with the models produced in laboratory tests, could offer a means of monitoring corrosion levels, as well as rock rib deformation.

Introduction

Reducing the number of rock fall injuries and fatalities is an important part of the mission of the National Institute for Occupational Safety and Health (NIOSH) Spokane Mining Research Division (SMRD). Ground control using support systems to protect miners from rock falls is one of the oldest mining sciences, and considerable research has led to a variety of modern tools and methods in use today. Among these tools are rock bolts and welded-wire mesh, which are made from increasingly higher-strength steel grades to meet the increasingly demanding requirements of underground mines [1]. However, the benefits of these higher-quality support elements may be negated in

corrosive mining environments. A better understanding of how corrosion affects the support capacity of ground support systems will assist engineers in determining when an opening is at a greater risk of falls of ground.

Accelerated corrosion has been occurring in some areas of the Hecla Mining Company's Greens Creek Mine near Juneau, Alaska, USA. Corrosion of ground support has resulted in two falls of ground occurring between April 2015 and March 2016. While these falls of ground did not injure any personnel, mine management recognized the high risk to miner safety and responded by actively undertaking a ground support rehabilitation program. Rehabilitation measures include the installation of both galvanized and coated, corrosion-resistant bolts and welded-wire mesh, depending on local conditions.

Prior to the first fall of ground, Hecla initiated a cooperative research study with SMRD to investigate the underlying mechanisms of ground support corrosion at the Greens Creek Mine, identify contributing factors, devise methods for assessing and monitoring the extent of corrosion on ground support elements, and develop practical solutions to the problem. SMRD researchers travelled to the Greens Creek Mine to collect samples and conduct field studies. Rock, welded-wire mesh, and rock bolt samples exposed to corrosive and non-corrosive environments were provided by Greens Creek personnel, while Dywidag-Systems International (DSI) supplied new welded-wire mesh and rock bolt samples for use in this study. This paper summarizes some of the results obtained in the first year of this project—namely, possible corrosion monitoring methods and the effect corrosion has on ground support integrity.

Background

Sulfur mineralogy influences the corrosivity of mine environments (see, for example, Hassell et al. [2]). The Greens Creek Mine orebody is a polymetallic massive sulfide deposit mined for its silver, zinc, gold, and lead. Major sulfide minerals include pyrite, sphalerite, galena,

and tetrahedrite/tennantite. Mineralization occurs discontinuously along the contact between a structural hanging wall (quartz mica carbonate phyllites) and footwall (graphitic and calcareous argillite). The high rate of corrosion is most apparent in ground support in contact with the dark-colored graphitic argillite footwall (Figure 1).



Figure 1. Galvanic corrosion of welded-wire mesh in contact with argillite rock mass.

A comprehensive research regimen was developed based on these initial field observations. Field components included surveys of welded-wire mesh corrosion, photogrammetric surveys, and rock mass conductivity measurements. Laboratory testing consisted of tension testing of welded-wire mesh samples, and analyses of both rock and welded-wire mesh samples using a Scanning Electron Microscope (SEM), Energy Dispersive Spectrometry (EDS), and Fourier Transform Infrared Spectrometry (FTIR). This paper focuses on the results obtained in photogrammetric surveys and laboratory tension tests. The possibility of combining these results to assess ground support integrity is discussed.

Photogrammetry Methodology

Photogrammetry background

Photogrammetry is the process of capturing three-dimensional geometry through photography (Figure 2). This technology has been successfully implemented for geometric and spatial analyses in numerous industries, including surveillance, law enforcement, transportation, manufacturing, materials testing, and medicine. Data collection may take as little as a few minutes, can be performed at safe distances from hazardous conditions, and can capture complete geometry for future laboratory analysis. Applied to underground mining, photogrammetry provides the opportunity to develop a visual history of ground support that can help in assessing the progress of corrosion, cracking, bagging, etc., and projecting when rehabilitation might be required to maintain ground safety. Using photogrammetry, SMRD researchers have achieved measurement accuracies within 1.0 mm in both field and laboratory settings [3-5]. SMRD photogrammetry work at

the Greens Creek Mine specifically involves monitoring the geometric change of installed welded-wire mesh during corrosion.



Figure 2. A 3D point cloud generated from a digital photograph pair (top), connected by a triangulated mesh (center), overlain by photographic texture data (bottom).

Mine personnel and SMRD researchers selected two characteristic areas of the mine for photogrammetry study. These areas representing “high corrosion” and “control”, were scrutinized for any key components that may have effects on corrosion, including rock mass conductivity, atmospheric conditions, and ground support histories. The high-corrosion site—M 390, a ventilation and exploration drift—is shown in Figure 3, while the control area—raise access PD 2853—is shown in Figure 4. Comparison of welded-wire mesh geometries in the two locations over time assumed any changes were due to corrosion only.

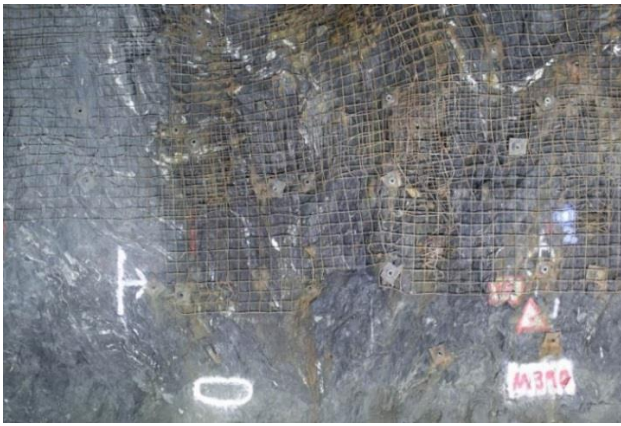


Figure 3. M 390, representing an area with high visual corrosion in dark argillite rock mass.



Figure 4. PD 2853, representing the control area with little to no visual corrosion in phyllite rock mass.

A survey of twenty-four photographs were taken at each site using the light and camera plan view shown in Figure 5. In the figure, the thin blue arrows represent the camera direction for each of the six camera stations. Four photographs were taken at each station—two in the direction of each arrow. The camera was rotated on a tripod to take the sequence of pictures required while the three lighting units remained stationary throughout each survey. To calibrate and map the mine excavation, three control points were placed on the rib at each site, represented by red dots in Figure 5. Each survey took approximately twenty minutes to conduct. Image resolution for the control site was 5.8 mm/pix, with a survey error of 3.3 mm. The high-corrosion site's image resolution was poor at 11.4 mm/pix, with a survey error of 4.7 mm. This could be improved in by positioning the camera closer to the rib or by using a higher resolution camera. Short range laboratory photogrammetric surveys achieved a survey error of 1.1 mm with a resolution of 0.6 mm/pix. In an attempt to catalog geometric change only due to corrosion, undistorted sections of mesh were chosen at each survey site for measurement.

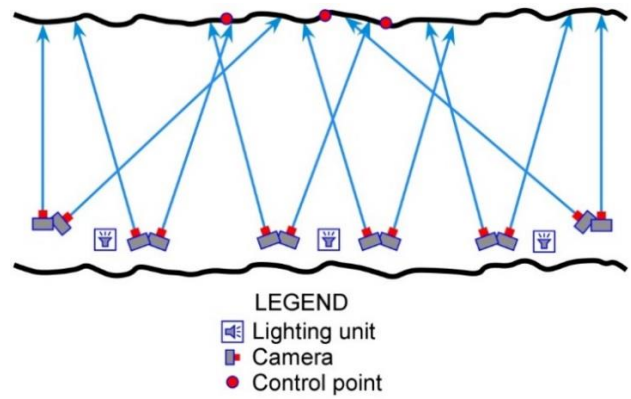


Figure 5. Plan view of Greens Creek Mine photogrammetry survey, showing camera positions, lights, and control points. Tunnel width for both survey sites was typically about 15 feet.

Photogrammetry Results and Discussion

Three types of measurements were made at each survey site: single-wire width (t), wire-to-wire distance (w), and diagonal distance between welds (d) (Figure 6). Wire strands at the high-corrosion survey site had undergone bulking, resulting in larger wire width measurements ($t + \Delta t$) than strands at the survey control site. Geometrically, wire, wire-to-wire and diagonal measurements were less ($w - \Delta w$ and $d - \Delta d$, respectively) for the high-corrosion site than for the control due to thicker strands being closer to each other in the mesh. Such a selection for the control site is shown in Figure 7.

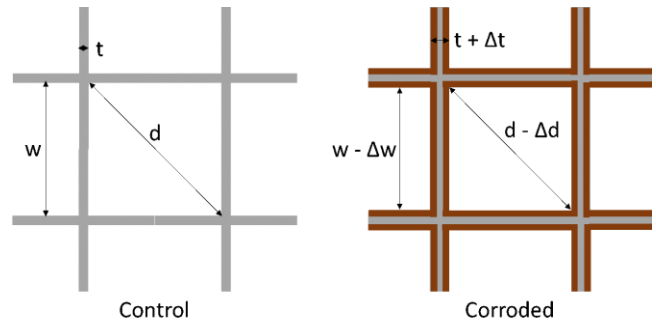


Figure 6. Conceptual diagram of geometric change in early-stage corroded welded-wire mesh section versus control. Gray represents original mesh while brown represents oxidized coating that develops due to corrosion.

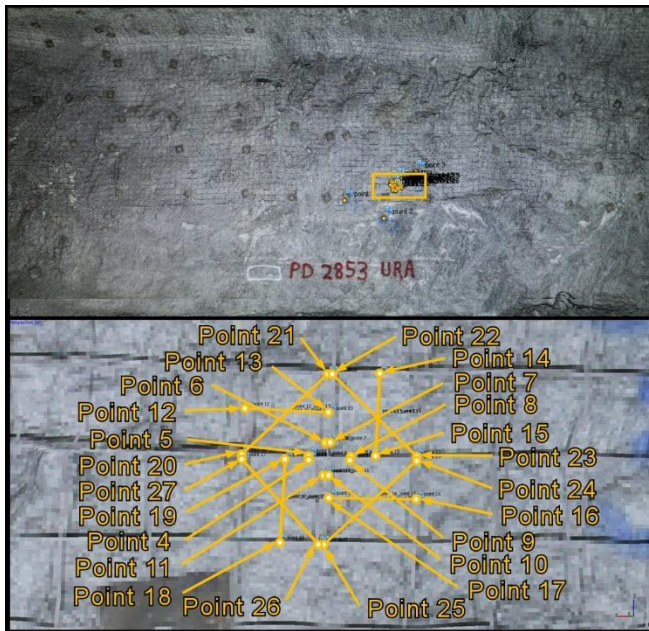


Figure 7. Corrosion control site at Green's Creek Mine (top), zoomed in to the area selected for photogrammetric measurement (bottom).

To determine how well changes in mesh geometry can be tracked over time using photogrammetry, data from both December 2015 and May 2016 were analyzed. Measurements of single-wire width, wire-to-wire distance, and diagonal distance between welds suggested bulking of the wire. Bulking of the wire strands suggests the buildup of oxidized metal. These measurements are summarized in Table 1. Additionally, the measurements indicated a continued buildup of oxidized materials on the welded-wire mesh during the time frame of study—December 2015 to May 2016—indicating that photogrammetry may be able to track corrosive progression, as well as providing a means of comparing corroded to non-corroded ground control materials to one another.

Table 1. Summary of measurements taken at the Green's Creek Mine to determine the ability of photogrammetric methods to track corrosion of support material.

PHOTOGRAMMETRIC MEASUREMENTS OF CORROSION	
Dec 2015	Δd corroded and control site
Single-wire width	+ 1.2 mm
Wire-to-wire distance	-2.4 mm
Diagonal distance	-4.5 mm
May 2016	Δd corroded and control site
Single-wire width	+1.9 mm
Wire-to-wire distance	-4.9 mm
Diagonal distance	-5.8 mm

Photogrammetric methods may be used to estimate the thickness of welded-wire mesh used for ground control in underground mining. Differences in thickness should be regarded as qualitative rather than quantitative because of the uncertainty in the measurement. Time-lapse comparisons have indicated the possibility of estimating geometric change over time. Disintegration of welded-wire mesh has not yet been observed in photogrammetric surveying, this could be due to the large uncertainty in the measurements. Higher resolution cameras may increase the capability of corrosion monitoring.

Oxidized metal causing wire bulking may hide the effective diameter of the welded-wire mesh, potentially leading miners to believe the ground support is intact when it has in fact lost support capacity. A preliminary study of the relationship of the bulked and the effective diameter of welded-wire mesh samples has been conducted as well as a study of the effect of the loss of diameter due to corrosion on support capacity. Understanding the relationship of bulked to effective diameter and the relationship of effective diameter to support capacity will help determine if photogrammetry can be used as a tool to estimate support capacity.

Corrosion Cycle

At the onset of corrosion the metal appears to expand or bulk as the corrosion product forms. In the case of welded-wire mesh the effective diameter of the wire may be much less than it appears. Figure 8 shows a sample before and after removal of the corrosion product. The sample experienced total removal on only half of the sample to show the bulking due to buildup of corrosion product.



Figure 8. Top: before cleaning the sample measured 7.27 mm. Bottom: after cleaning the sample measured 4.20 mm.

The diameter of the sample shown in Figure 8 was measured in the laboratory prior to and after multiple cleaning cycles following ASTM G1-03 [6]. The final cleaning cycle was performed with sandblasting (Figure 9).

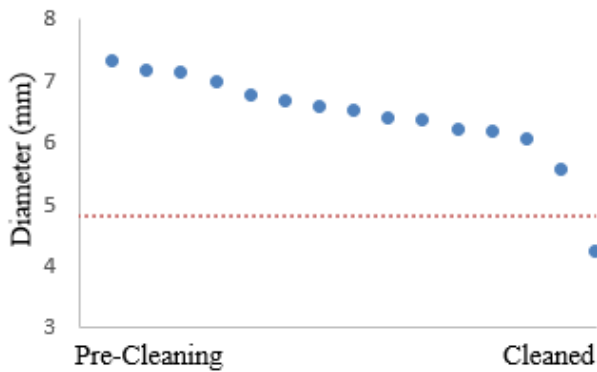


Figure 9. Change in diameter with multiple cleaning cycles – final cleaning cycle was sand blasted. The dashed line represents the original diameter of the sample.

Apparent bulking has been estimated by photogrammetric measurements in the range of 25 – 40% greater than the original diameter. Continued corrosion may result in weakly attached product which begins to flake off. Maximum bulking is determined, in part, by any vibrations, abrasions, etc. that the wire is subjected to. Initial observations in the laboratory suggest bulking of as much as 73%. Flaking, or cleaning with a wire brush, were observed to reduce total diameter to metal and corrosion products which are well attached to the metal. These can be removed by acid washing, leaving an un-corroded wire which provides the effective strength of the corroded mesh. Figure 10 demonstrates the relationship of corroded wire diameter to the wire diameter under the layer of corrosion product for the initial set of samples taken from a small test section. This observation applies to this small sample set and may be different for samples exposed to differing types of corrosion.

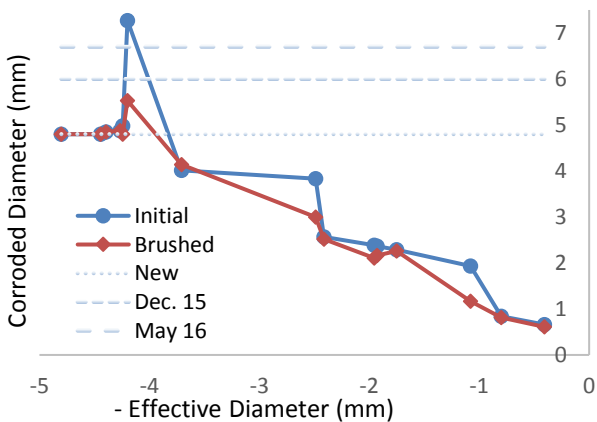


Figure 10. Corroded wire diameter as a function of wire diameter (sign changed). Lines represent the diameter of new mesh and the diameters estimated using photogrammetry in December 2015 and May 2016.

Further testing will seek to fill in gaps in this relationship. These tests will start with photogrammetry surveys to establish apparent diameter of a sample in situ, then the mesh will be sampled and the diameter of loose and tight corrosion shells measured. Finally, the surviving wire

strand will be tested for tensile strength. If consistent relationships can be established, the tensile strength of corroded wire mesh can be estimated from photo pairs (which can be taken quickly and easily—especially compared to lab testing).

Tension Test Methodology

Wire Tension test

Tension pull tests of the welded-wire mesh samples were conducted using a 12 kip Tinius Universal Testing Machine following ASTM E8/E8M-11 [7]. A section of the welded-wire mesh was cut, then the minimum diameter was measured to achieve statistical average. The minimum diameter was recorded because this is where the mesh is expected to break [8]. The testing zone of the sample was in the center of the wire; in this zone the sample was marked at two sites two inches apart. The samples were secured in the Tinius instrument using pull claw attachments and subjected to a load rate of 150 lbs/sec (Figure 11). After the sample failed, elongation was found by fitting the broken pieces together and measuring the final distance between the two marked sites. The elongation measurement was used to calculate the nominal strain of the sample.



Figure 11. A welded-wire mesh sample being pulled at 150 lbs/sec until breaking.

Weld Tension test

Weld tension tests were conducted to compare the strength of the weld, the wire, and the heat affected zone (HAZ) [9] (Figure 12). A perfect weld should be stronger than the wire itself. These tests were carried out according to ASTM A497/A497-07 [10].

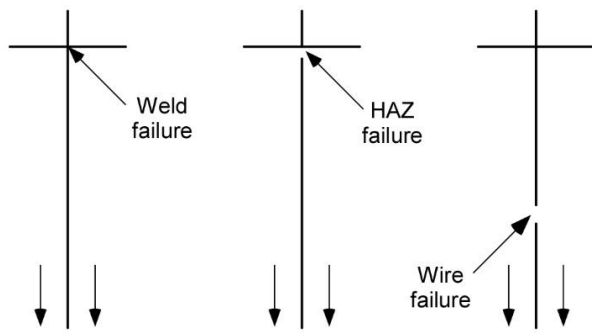


Figure 12. Mode of failure in the weld, the heat affected zone (HAZ), and the wire after [9].

Sections of wire were again cut from the samples provided by the Greens Creek Mine. Villaescusa [9] reported a slight difference in failure mode in the longitudinal wire compared to the cross wire in weld, therefore, in this study two samples with different orientation were cut and both were tested. Again the thinnest part of the sample was chosen for testing because this is the most likely location of failure. Some samples included welds that had already separated due to corrosion, in these instances the thinnest section that could be fit into the test apparatus was chosen. Orientation is not noted in the sample pairs because the samples from the mine do not indicate orientation. The same 12 kip Tinius Universal Testing Machine was used with a different attachment. Figure 13 shows a schematic of the apparatus and its main functional components. The sample is pulled from the bottom, putting stress on the weld at 150 lbs/sec until failure occurs. Samples that failed in the wire rather than the weld were included in the data of the wire tension tests.

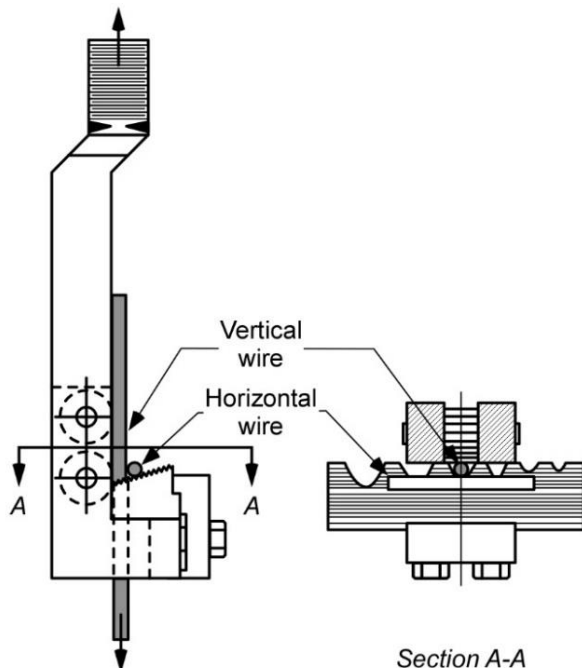


Figure 13. Welded-wire reinforcement weld tester after ASTM A497/A497M-07 [10].

Tension Test Results

Wire Tension test

A positive exponential relationship was observed between the maximum load before failure and the measured diameter of the welded-wire mesh (Figure 8). Dorion, et al. [8] observed a similar exponential relationship with welded-wire mesh samples also obtained from a mining environment. The differences in the mathematical relationship observed by Dorion, et al. ($Failure\ Load\ (kN) = 0.38 \times d^{2.2}$) and this study (Figure 14) could be due to the differences in number of samples or variations in the metallic properties of the welded-wire mesh. Analysis by Dorion et al. and SMRD both come close to the diameter squared relationship that results from a change in strand diameter. Samples around 3.5 mm diameter have lost roughly half their strength, this could be a valuable threshold for significant strength loss. In Figure 10, 3.5 mm diameter correlates to samples that are no longer bulked and would appear in a mining environment to have a slightly smaller diameter than new welded-wire mesh.

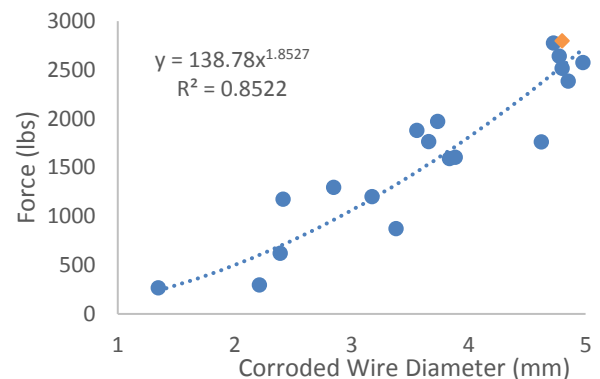


Figure 14. Welded-wire mesh failure load as a function of diameter in wire tension testing with the new welded-wire mesh represented by an orange diamond marker.

Nominal strain was calculated (equation 3) and compared to the diameter of the samples tested (Figure 15). Data indicates that there is a relationship between nominal strain and diameter for this sample set. The relationship indicates that loss in diameter due to corrosion causes embrittlement of the welded-wire mesh, that is, the material is less prone to stretch as load is applied. This is important as it reduces the robustness of the support (ability to maintain support safety through ground deformations).

$$Strain = \frac{\Delta length}{original\ length} \quad (3)$$

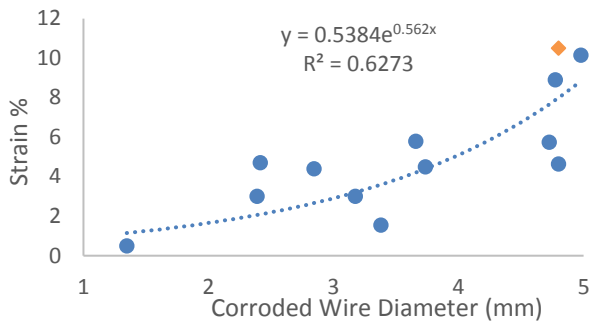


Figure 15. Nominal strain is lower in samples that have experienced a loss in diameter due to corrosion - the new welded-wire mesh is represented by an orange diamond marker.

Weld Tension test

The variability of mode of failure in the sample pairs is shown in Figure 16. From the tested samples, 57% of sample pairs failed in different ways depending on the orientation. The new welded-wire mesh sample failed in the HAZ for both orientations (Figure 16, sample number 14).

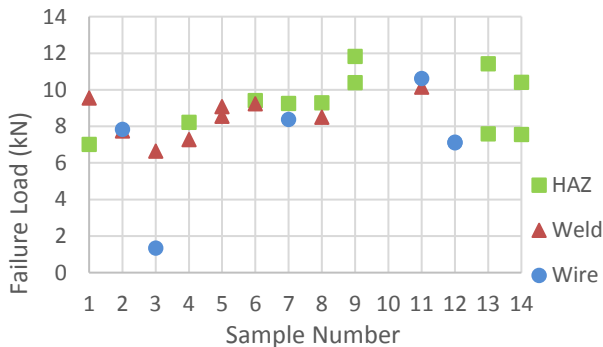


Figure 16. Mode of failure for the heat effected zone (HAZ), weld, and wire for each sample pair. Sample 14 is the new welded-wire mesh.

Table 2 gives the percentage of the total samples tested that failed in each of the three modes of failure investigated. The highest percentage of samples failed in the HAZ. This suggests the welding process may render the weld and HAZ more susceptible to corrosion. Further investigation of weld, HAZ, and wire metallurgy is needed to confirm this observation. The testing apparatus required sufficient wire length to secure the wire for the test; therefore in some cases the locations with the greatest corrosion could not be tested. A few samples with corroded welds experienced wire separation without any laboratory testing.

Table 2. Mode of failure of samples tested. The heat affected zone (HAZ), weld or wire.

Mode of Failure	% samples failed
HAZ	42%
Weld	35%
Wire	23%

Conclusions

Photogrammetric surveys may provide qualitative analysis of the bulking of welded-wire mesh as corrosion products form. A higher resolution camera or different camera positioning techniques could reduce the uncertainty in wire diameter measurements. Initial investigation of the relationship of the bulking from corrosion products and the loss of wire diameter indicate 2 mm bulking associated with roughly 0.5 mm effective metal diameter loss. A better understanding of the relationship between apparent diameter and the effective diameter could allow the use of photogrammetric surveys as a tool to monitor the support capacity, while also monitoring rock mass movement.

Samples taken from a mining environment were tested to better understand the effect of corrosion on the support integrity of the welded-wire mesh. An exponential relationship was observed between the breaking force and the effective diameter of the welded-wire mesh samples. The relationship between diameter loss due to corrosion and the nominal strain to failure indicated that welded-wire mesh becomes more brittle as the effective diameter decreases. Monitoring the diameter of the welded-wire mesh could give engineers an indication of the integrity of their ground support allowing them to identify potentially hazardous areas and plan rehabilitation accordingly.

Further testing will seek to understand the relationship between bulked diameter, effective diameter, and strength. These tests will start with photogrammetry surveys to establish the apparent diameter of a sample in situ, then the mesh will be sampled and the diameter of loose and tight bulked diameter measured. Finally, the surviving wire strand will be tested for tensile strength. If consistent relationships can be established, the tensile strength of corroded wire mesh can be estimated from photo pairs, which can be taken quickly and easily—especially compared to lab testing.

Acknowledgements

Much of this research took place in the Greens Creek Mine. SMRD would like to thank Mark Board for initiating this project and for his continued support. The work and cooperation of the miners and engineers at Hecla Mining Company is very much appreciated. SMRD would like to thank DSI for providing welded-wire mesh and bolt samples.

Disclaimer

Use of trade names and commercial sources is for identification only and does not imply endorsement by NIOSH, the Centers for Disease Control and Prevention, or the U.S. Department of Health and Human Services. The findings and conclusions in this report are those of the authors and do not necessarily represent the official position of NIOSH, the Centers for Disease Control and Prevention, or the U.S. Department of Health and Human Services.

References

1. Elias, E., Vandermaat, D., Craig, P., Chen, H., Crosky, A., Saydam, S., Hagan, P. and Hebblewhite, B. (2013). Metallurgical examination of rockbolts failed in service due to stress corrosion cracking. *7th International Symposium on Ground Support in Mining and Underground Construction*, Perth, Western Australia, Australia, Australian Centre for Geomechanics. 473-483.
2. Hassell, R., Villaescusa, E., Thompson, A.G. and Kinsella, B. (2004). Corrosion assessment of ground support systems. London, Taylor & Francis Group. 529-542.
3. Benton, D.J., Iverson, S.R., Johnson, J.C. and Martin, L.A. (2014). Photogrammetric Monitoring of Rock Mass Behavior in Deep Vein Mining. *33rd International Conference on Ground Control in Mining*, Morgantown, WV. 7.
4. Benton, D.J., Boltz, M.S., Raffaldi, M.J. and Iverson, S.R.(2015) Using Photogrammetry to Monitor Underground Mining Environments. ARMA e-Newsletter Special Issue: Imaging and Remote Sensing in Rock Mechanics 11-16
5. Benton, D.J., Iverson, S.R., Martin, L.A., Johnson, J.C. and Raffaldi, M.J. (2015). Volumetric Measurement of Rock Movement Using Photogrammetry. *34th International Conference on Ground Control in Mining*, Morgantown, WV. 9.
6. ASTM G1 - 03 (2011) Standard Practice for Preparing, Cleaning, and Evaluation Corrosion Test Specimens. West Conshohocken, PA. American Society for Testing and Materials. 8.
7. ASTM E8/E8M-11 (2011) Standard Test Methods for Tension Testing of Metallic Materials. West Conshohocken, PA. American Society for Testing and Materials.
8. Dorion, J.F., Hadjigeorgiou, J. and Gahli, E. (2015). Quantifying losses in support capacity due to corrosion. *CIM Journal* 6(3): 9.
9. Villaescusa, E. (1999). Laboratory testing of weld mesh for rock support. *International Symposium on Ground Support*, Kalgoorlie, Western Australia A.A. Balkema. 155 - 159.
10. ASTM A497/A497M-07 (2007) Standard Specification for Steel Welded Wire Reinforcement, Deformed, for Concrete. West Conshohocken, PA. American Society for Testing and Materials.